Oxovanadium(IV) complexes bearing substituted pentane-2,4-dionate ligands: Synthesis, structure and drying activity in solvent-borne alkyd paints.

Ondřej Preininger [a], Iva Charamzová [a], Jaromír Vinklárek [b], Ivana Císařová [c], Jan Honzíček [a,*]

[a] Institute of Chemistry and Technology of Macromolecular Materials, Faculty of Chemical Technology, University of Pardubice, Studentská 573, 532 10 Pardubice, Czech Republic.

[b] Department of General and Inorganic Chemistry, Faculty of Chemical Technology, University of Pardubice, Studentská 573, 532 10 Pardubice, Czech Republic.

[c] Department of Inorganic Chemistry, Faculty of Science, Charles University in Prague, Hlavova 2030/8, 128 43 Prague 2, Czech Republic.

∗ Corresponding author. Tel.: +420 46603 7229; fax: +420 46603 7068.

E-mail address: jan.honzicek@upce.cz (J. Honzíček).

Keywords: vanadium; acetylacetonate; X-ray structure; alkyd paints; autoxidation

Graphical abstract:

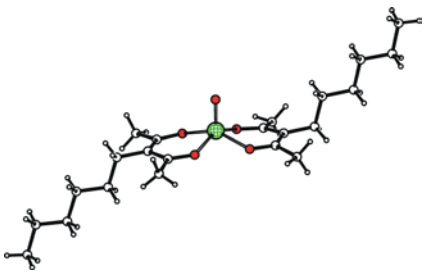

Highlights:

Oxovanadium(IV) compounds with increased solubility were prepared.

X-ray structures of title compounds were determined.

Catalytic activity was established on solvent-borne alkyd paints.

The activity was studied mechanical tests and infrared spectroscopy.

Abstract

New oxovanadium(IV) pentane-2,4-dionate complexes decorated with long alkyl tails have been prepared and characterized by the spectroscopic methods and the X-ray crystallography. The increased solubility in non-polar organic solvents enabled to investigate the catalytic activity of the title compounds on various solvent-borne alkyd resins. The detailed study of the drying process reveals their excellent performance at considerably lower concentrations than usual for commertial cobalt-based driers. Furthermore, the oxovanadium(IV) compounds are highly active in wider range of concentration. Such lower sensitivity to precise dosage helps to avoid the overdose effect without necessity of other additives.

1. Introduction

Alkyd resins modified with unsaturated fatty acids have been established as a significant group of air-drying paints used in modern organic coatings. Presence of double bonds in the fatty acid tails enables the reaction with air oxygen to give three-dimensional polymeric structure. This radical process, called autoxidation, converts the liquid paint layer to the firm coating [1]. The alkyd resins are able to provide polymeric film without addition of any curing agents but this process is at ambient temperature very slow giving the paint film with low final hardness. Nevertheless, the use of metal catalysts, so-called driers, significantly reduces the drying time and improves physical properties of resulting polymeric film [2, 3].

The quest for new and powerful alkyd driers, suitable for paint producing industry, is stimulated by European REACH (Registration, Evaluation, Authorisation and Restriction of Chemicals) legislation since well-established cobalt-based driers (*e.g.* cobalt(II) 2-ethylhexanoate; **Co-Nuodex**) are under evaluation by European Chemical Agency. In 2012, the cobalt(II) carboxylates have been classified as "CMR2-Reprotoxic" by the Cobalt REACH Consortium and may be in near future reclassified to carcinogenic class 1B, which would restrict their use. Although autoxidation is catalyzed by various manganese [4-8], iron [8-11] and vanadium complexes [12, 13], most of them still suffers from several disadvantages such as low activity at ambient temperature, intense coloration or low solubility in alkyd binder [14].

The aim of this study is to design series of new oxovanadium compounds with increased solubility in non-polar solvents. This target will be achieved by attachment of linear alkyl tails on pentane-2,4-dionate ligands of $[VO(acac)_2]$ (acac = *O*,*O*-MeCOCHCOMe). Catalytic activity of these complexes will be established on solvent-borne alkyd resins of different oil length using standard mechanic tests and time-resolved infrared spectroscopy.

2. Results and discussion

2.1 Synthesis of oxovanadium(IV) complexes.

A series of the substituted pentane-2,4-diones, decorated with alkyl chains in 3-position (**1a**–**1c**), was synthesized using reaction of alkyl iodide and pentane-2,4-dione under basic conditions. The starting alkyl iodides are formed *in situ* from readily available alkyl bromide and sodium iodide in acetone, see Scheme 1.

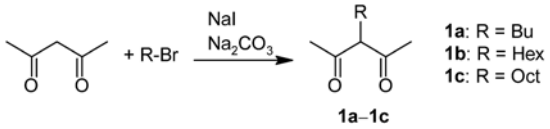

Scheme 1. Synthesis of substituted pentane-2,4-diones.

The reaction of the β-diketones **1a**–**1c** with aqueous solution of oxovanadium sulfate gives upon neutralization the oxovanadium compounds **2a**–**2c**, respectively. The yield of the reaction strongly depends on purity of the starting oxovanadium sulfate. The reproducible yields (~50%) were obtained only when residual sulfuric acid is removed from crude oxovanadium sulfate by multiple extractions with acetonitrile. The impurities in crude oxovanadium sulfate probably strongly influence the speciation of the aqueous solution, which is very pH sensitive [15].

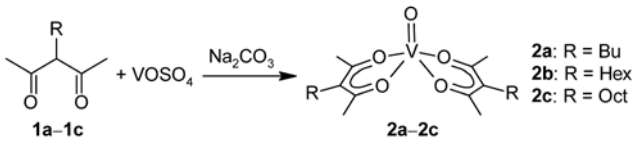

Scheme 2. Synthesis of oxovanadium complexes.

The complexes **2a**–**2c** are paramagnetic making characterization by routine NMR spectroscopy quite difficult. Nevertheless, these d^1-complexes are amenable for EPR spectroscopic characterization. The solution spectra, collected at room temperature in toluene, show expected eight-line isotropic pattern due to hyperfine interaction with vanadium nucleus (^{51}V; $I = {}^7/_2$; 99.8 %). The compounds **2a**–**2c** show lower value of isotropic hyperfine coupling constant ($|A_{iso}| \sim 104.2 \times 10^{-4}$ T) and lower isotropic *g*-factor ($g_{iso} \sim 1.948$) than unsubstituted analogue [VO(acac)$_2$] ($|A_{iso}| = 108.7 \times 10^{-4}$ T, $g_{iso} = 1.969$) [12]. It reveals higher delocalization of the unpaired electron on ligands, which is probably due to electron releasing properties of alkyl groups that lowers the ionic character of the V–O bonds. Anisotropic spectra, obtained from frozen toluene solutions, are rhombic symmetric that is in line with expected C_{2v} symmetry of the compounds. The components of the *A*-tensor and *g*-tensor are not affected by length of the alkyl tail ($|A_z| \sim 186.5 \times 10^{-4}$ T, $|A_y| \sim 66.6 \times 10^{-4}$ T, $|A_x| \sim 56.5 \times 10^{-4}$ T, $g_z = 1.935$, $g_y = 1.973$, $g_x = 1.969$). Infrared spectra of **2a**–**2c** show band of medium intensity at ~995 cm^{-1} that was assigned to V=O stretching.

*2.2 X-ray structures of [VO(3-Bu-acac)$_2$](**2a**), [VO(3-Hex-acac)$_2$](**2b**) and [VO(3-Oct-acac)$_2$] (**2c**)*

Structures of the oxovanadium compounds **2a**–**2c** were determined by the single crystal X-ray diffraction analysis. The bond lengths and bond angles, describing coordination sphere of central metal, are summarized in Table 2. The compounds **2a**–**2c** are mononuclear species with approximate C_{2v} point group symmetry. The coordination sphere of vanadium forms a distorted square pyramid with terminal oxygen atom in apical position. The basal plane is formed by oxygen donor atoms of two substituted pentane-2,4-dionates (Figs. 1–3). The V=O bond is nearly perpendicular to the basal plane (see α in Table 1) and vanadium atom lies ~0.55 Å above it (see *d* in Table 1). The here presented modification of the penta-2,4-dionate ligand has only minor effect on coordination sphere of vanadium as evident from very similar values of structural parameter given in Table 1 for the compounds **2a**–**2c** and previously reported analogues [VO(acac)$_2$] [16], [VO(3-Me-acac)$_2$] [17] and [VO(3-Et-acac)$_2$] [17]. The most relevant distortion from parent [VO(acac)$_2$] is considerably smaller dihedral angel between planes of the pentane-2,4-dionate ligands (see β in Table 1) that is probably due to weak intermolecular interactions in crystal lattice.

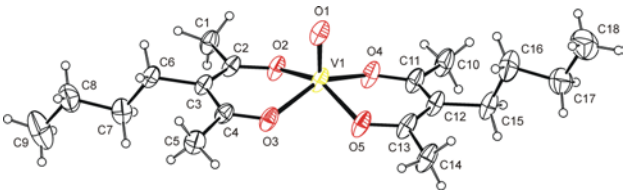

Fig. 1. ORTEP drawing of the molecule **2a**. The labeling scheme for all non-hydrogen atoms is shown. Thermal ellipsoids are drawn at the 50% probability level. One position of disordered atoms is omitted for clarity.

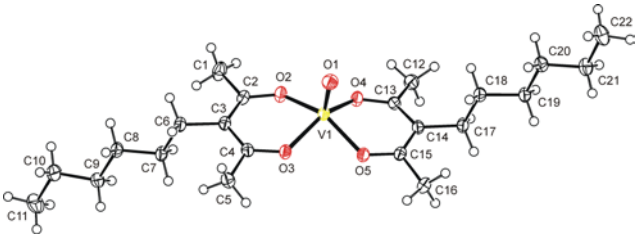

Fig. 2. ORTEP drawing of the molecule **2b**. The labeling scheme for all non-hydrogen atoms is shown. Thermal ellipsoids are drawn at the 30% probability level.

Table 1. Selected bond lenghts (Å) and bond angles (°) for the compounds **2a**–**2c**.

	2a	**2b**	**2c**	$[VO(acac)_2]$ [d]	$[VO(3\text{-Me-acac})_2]$ [e]	$[VO(3\text{-Et-acac})_2]$ [e,f]
V1–O1	1.586(2)	1.5925(9)	1.5905(13)	1.584(2)	1.592(2)	1.605(2)
V1–O2	1.9612(17)	1.9642(9)	1.9642(11)	1.967(1)	1.968(2)	1.962(2)
V1–O3	1.9574(19)	1.9644(9)	1.9647(12)	1.969(1)	1.971(2)	1.965(2)
V1–O4	1.9521(17)	1.9594(9)	1.9561(11)	1.970(1)	1.958(2)	1.962(2)
V1–O5	1.9553(17)	1.9586(8)	1.9569(11)	1.968(1)	1.956(2)	1.966(2)
O2–V1–O3	85.24(7)	85.65(4)	85.50(5)	87.59(5)	85.58(7)	85.74(7)
O4–V1–O5	85.72(7)	85.46(4)	85.92(5)	87.29(6)	86.25(7)	85.59(7)
O2–V1–O4	86.52(7)	84.15(4)	88.00(5)	83.80(6)	85.07(7)	84.75(7)
O3–V1–O5	84.55(7)	85.84(4)	82.56(5)	83.84(6)	84.25(7)	85.65(7)
α [a]	89.34(9)	89.00(5)	88.84(6)	89.91(6)	– [g]	– [g]
β [b]	4.04(13)	3.77(6)	0.76(8)	17.81(10)	– [g]	– [g]
d [c]	0.548(1)	0.563(1)	0.549(1)	0.5447(4)	0.55	0.56

[a] α is the angle between V1–O1 bond and mean plane of the basal oxygen atoms (O2, O3, O4 and O5); [b] β represents the dihedral angle between planes of the pentane-2,4-dionate ligands. The plane of the ligand is defined as the mean plane of oxygen and carbon atoms of the chelate ring; [c] *d* is defined as the distance between vanadium atom and mean plane of the basal oxygen atoms (O2, O3, O4 and O5); [d] data reported in literature [16]; [e] data reported in literature [17]; [f] Only data for one of two crystallographically independent molecules in the unit cell are given; [g] Not reported.

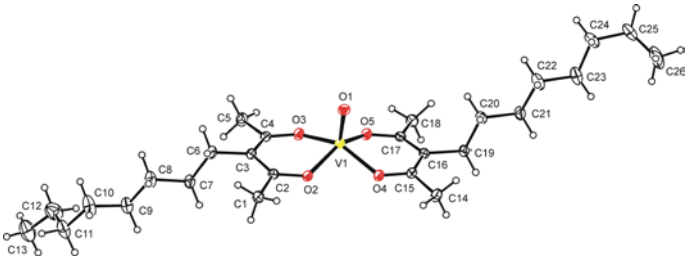

Fig. 3. ORTEP drawing of the molecule **2c**. The labeling scheme for all non-hydrogen atoms is shown. Thermal ellipsoids are drawn at the 30% probability level. One position of disordered atoms is omitted for clarity.

2.3 Drying activity of oxovanadium(IV) complexes.

High solubility of the compounds **2a**–**2c** in non-polar solvents such as toluene and xylene enables to study their drying activity on various solvent-borne air-drying paints. This study involves three alkyd resins modified with soybean oil. The selected resins of short (**S40**), medium (**S50**) and long oil length (**S60**) are representatives of the most common types of solvent borne alkyds used in paint-producing industry; see Scheme 3.

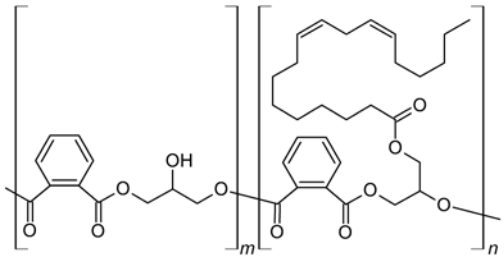

Scheme 3. Simplified structure of alkyd resin. Tail of linoleic acid is shown as a representative of a fatty acid suitable for autoxidation drying. The ratio *m* : *n* defines the oil length of the alkyd binder [18].

In order to optimize dosage of the vanadium compounds, mechanical properties of test coatings were examined in wide range of metal concentrations. The measurements of drying time and film hardness development were performed at metal concentration 0.005–0.03 wt.% (**S40**) or 0.005–0.1 wt.% (**S50** and **S60**). The optimal performance of the compounds **2a**–**2c** was observed at 0.03 wt.% of the metal in dry matter content. Hence, the total dry times (τ_2) do not exceed ten hours and further increase of concentration led only to its minor shortening (for full list of collected data given see Table S1 in Supplementary Material). The tack-free time (τ_1) and total dry time (τ_2) of the formulations containing the vanadium-based driers at optimal concentration are comparable or even shorter than observed for commercial **Co-Nuodex**, see Table 2. Measurements on the test coatings **S50** suggest similar curing properties as observed for parent complex [$VO(acac)_2$] [12]. Nevertheless, the activity in the other formulations (**S40** and **S60**) is very low owing to pure solubility. In this case, the attachment of long alkyl tails seems to be essential for application since solubility is the limiting factor. Formulations of the compounds **2a**–**2c** in **S50** show a fast rise of relative hardness in first few days of curing (Figure 4). Ten days after application, the vanadium compounds reach considerably higher value than **Co-Nuodex**, see $H_{rel;10d}$ in Table 2. This feature is of particular importance for application as it is closely related with scratch resistance of the protective coatings. Final hardness ($H_{rel;100d}$) of the test coatings treated with the vanadium compounds is generally lower than in the case of **Co-Nuodex** as evident mainly on coatings of the alkyd binders **S40** and **S60**. Nevertheless, the values are still satisfactory for common applications [1]. The final hardness of the test coatings can be easily increased up to level common for commertial **Co-Nuodex** by higher dosage of the drier. Hence, at metal concentration 0.1 wt.%, final hardness of the coatings treated with the vanadium driers and **Co-Nuodex** are comparable. We note that relative hardness of the test coatings is given mainly by properties of the structure units of given polymer. Therefore, the binders of the longer oil length usually give much softer coatings since the higher amount of the flexible fatty acid tails plasticizes the polymeric coating. In case of long-length alkyd binders, such as **S60**, the hard coatings could be reached only when the fatty acid tails are densely crosslinked.

Table 2. Drying times (τ), relative hardness (H_{rel}) and kinetic data of autoxidation process at optimal metal concentration. [a]

Formulation	τ_1 [b] (h)	τ_2 [c] (h)	$H_{rel;10d}$ [d] (%)	$H_{rel;100d}$ [e] (%)	$k_{CH,max}$ [f] (h^{-1})	t_{max} [f] (h)	IT [g] (h)	$t_{1/2}$ [h] (h)	t_{conj} [i] (h)
2a/S40	0.6	3.3	32.0	53.4	0.33	0.5	–	2.4	2.9
2b/S40	0.3	3.1	27.3	53.6	0.41	0.5	–	1.9	1.9
2c/S40	1.4	4.9	24.8	45.1	0.41	0.5	–	2.0	2.1
Co-Nuodex/S40 [j]	2.7	6.9	35.3	56.8	0.79	0.6	–	1.1	2.0
2a/S50	2.5	8.5	23.8	45.0	0.25	2.0	0.9	4.1	4.6
2b/S50	2.0	5.0	26.9	51.2	0.31	1.4	0.7	3.0	3.1
2c/S50	1.0	3.2	30.0	48.5	0.28	1.5	0.7	3.7	4.0
[$VO(acac)_2$]/**S50** [k]	1.1	6.5	32.3	47.9	0.38	0.6	–	– [l]	5.3
Co-Nuodex/S50 [j]	5.2	6.7	20.7	52.1	1.39	1.4	0.5	1.2	2.4
2a/S60	1.0	5.1	16.2	34.5	0.34	0.4	–	2.6	3.5
2b/S60	1.0	6.2	17.6	36.0	0.41	0.3	–	2.2	2.6
2c/S60	1.2	4.2	16.5	34.3	0.38	0.5	–	2.2	3.1
Co-Nuodex/S60 [j]	0.8	4.6	26.3	48.6	1.56	0.6	–	0.7	1.4

[a] Performance of vanadium-based driers at metal concentration 0.03 wt.% is compared with optimal concentration of cobalt-based drier (0.06 wt.% for **S40**, 0.1 wt.% for **S50** and **S60**); [b] Tack free time; [c] Total dry time; [d] Relative hardness after 10 days; [e] Relative hardness after 100 days; [f] Maximum oxidation rate constant ($k_{CH,max}$) observed at drying time t_{max}; [g] Induction time (*IT*) has been determined graphically as intersection of tangential lines extending the curve before and after knee point; [h] The time $t_{1/2}$ is determined as point when 50% of active CH bonds are consumed; [i] Drying time in which the band at 989 cm^{-1} reached maximal intensity; [j] Data reported in elsewhere [13]; [k] Data reported in elsewhere [12]; [j] |Not reported.

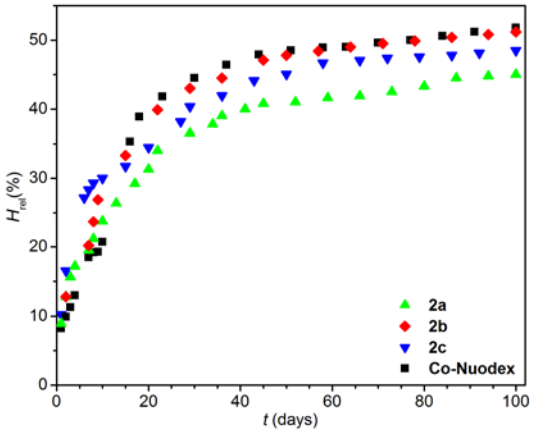

Fig. 4. Relative hardness development for formulations of alkyd binder **S50**.

2.4 In-situ FTIR spectroscopy

Time-resolved FTIR spectroscopy is routinely used on liquid model systems (*e.g.* ethyl linoleate or ethyl linolenate) to quantify the catalytic power of the autoxidation catalysts [19]. The development of the C–H stretching band at 3008 cm^{-1}, assigned to non-conjugated *cis*-CH=CH moiety [20], enables to follow disappearance of double allylic methylene that is the active moiety of alkyd resins modified with semi-drying oils (*e.g.* soybean or linseed oil) [21]. Recently, we have extended this method on the test alkyd coatings that enables to capture the differences in behavior of one catalyst in various alkyd formulations [11].

Figure 1 shows development of the band at 3008 cm^{-1} in time for alkyd resin **S50** treated with the compounds **2a**–**2c** and commertial **Co-Nuodex** at optimal concentration. The logarithmic plots of the vanadium compounds are linear up to 50% conversion with short induction times (0.7–0.9 h). Such behavior is common for reaction of pseudo-first order that occurs in liquid systems saturated with air oxygen. The maximal rate constants vary between 0.25 and 0.31 h^{-1} that is close to the value obtained for parent complex [$VO(acac)_2$] (0.38 h^{-1}). Although **Co-Nuodex** and vanadium compounds **2a**–**2c** show similar drying time τ_2 at optimal concentration, the maximal rate constant of the cobalt compound is considerably higher (1.39 h^{-1}). Such "virtual overdosing" by cobalt compound is probably the main reason for higher density of crosslinking on the upper surface of the coating. In this particular case, the autoxidation reaction consumes the air-oxygen much faster than it diffuses into the whole volume of the coating, which led to gradual drying from the upper surface. We note that such front-formation cannot be easily overcame by lower dosage of cobalt compound owing to long induction period at 0.03 wt.% (IT = 10h) [12] that deteriorates the drying performance. Fast front formation could be reduced only by additives known as through driers and auxiliary driers [2].

The measurements on compounds **2a**–**2c** in alkyd resins **S40** and **S60** reveal very similar catalytic activity as observed in resin **S50**. The rate coefficient of the hydrogen abstraction from double allylic moiety varies between

0.33 and 0.41 h^{-1} and induction times are negligible. Such behavior is very promising for application since polarity of alkyd binder has only minor effect on catalytic activity.

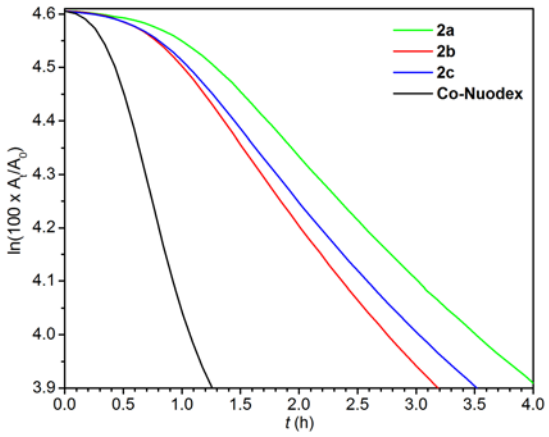

Fig. 5. Time dependent integral plots of the band at 3008 cm^{-1} for formulations of alkyd binder **S50** at optimal concentration. Only region of the up to 50% conversion is shown for clarity.

2.5 EPR spectra of dried films

Behavior of vanadium compounds **2a**–**2c** in alkyd resins **S40**, **S50** and **S60** was studied by EPR spectroscopy. Our experiments confirmed presence of vanadium(IV) species in the dried films two weeks after application but the spectra are different from those in frozen toluene solutions of **2a**–**2c** (Figure 6). The films, cured with the vanadium driers, give axial symmetric spectra with pattern typical for regular square-planar molecular structure. Furthermore, the components of *A*-tensor are considerably higher than observed for intact species **2a**–**2c**. The EPR parameters of the films are not affected by length of the alkyl tail on pentane-2,4-dionate ligand or the oil-length of the alkyd binder, see Table 3. Such observations imply that the compounds **2a**–**2c** are precursors of active vanadium(IV) species, which appears upon reaction with function groups on alkyd binder or air-oxygen. The molecular structure of the active species was not elucidated. Nevertheless, is seems to be the same as observed recently in formulations cured with oxovanadium(IV) 2-ethylhexanoate [13].

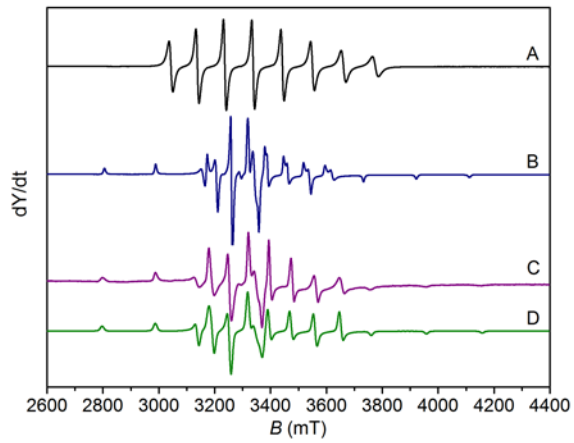

Fig. 6. EPR spectrum of: (A) toluene solution of **2a** at 293K, (B) toluene solution of **2a** at 123K, (C) alkyd layer cured with **2a**. (D) Computer simulation of the spectrum C.

Table 3. Hyperfine coupling constants (10^{-4} T) and *g*-factors of oxovanadium compounds.[a]

		$\lvert A_z \rvert$	$\lvert A_y \rvert$	$\lvert A_x \rvert$	g_z	g_y	g_x	$\lvert A_{iso} \rvert$ [b]	g_{iso} [b]
	toluene 293 K	–	–	–	–	–	–	104.2	1.948
	toluene 123 K	186.6	66.7	56.2	1.939	1.97	1.971	103.2	1.960
2a	**S40**	194.1	73.3	73.3	1.934	1.978	1.978	113.6	1.963
	S50	194.9	72.9	72.9	1.933	1.976	1.976	113.6	1.962
	S60	194.3	73.0	73.0	1.938	1.979	1.979	113.4	1.965
	toluene 293 K	–	–	–	–	–	–	104.4	1.949
	toluene 123 K	186.9	67.0	56.7	1.938	1.973	1.967	103.5	1.959
2b	**S40**	194.4	73.1	73.1	1.934	1.975	1.975	113.5	1.961
	S50	194.5	73.0	73.0	1.933	1.975	1.975	113.5	1.961
	S60	194.4	73.0	73.0	1.932	1.975	1.975	113.5	1.961
	toluene 293 K	–	–	–	–	–	–	104.2	1.948
	toluene 123 K	186.1	67.2	56.3	1.931	1.976	1.970	103.2	1.959
2c	**S40**	194.9	73.3	73.3	1.93	1.971	1.971	113.8	1.957
	S50	194.9	72.8	72.8	1.928	1.976	1.976	113.5	1.960
	S60	194.4	73.0	73.0	1.932	1.975	1.975	113.5	1.961

[a] The spectra were measured in fluid toluene solution (293 K), frozen toluene solution (123 K) and in dried alkyd resins **S40**, **S50** and **S60**. [b] In case of anisotropic spectra, the isotropic parameters were calculated using following equations: $|A_{iso}| = (|A_x| + |A_y| + |A_z|) / 3$; $g_{iso} = g_x + g_y + g_z) / 3$.

3. Conclusions

This study described synthesis, characterization and crystal structure of three new oxovanadium(IV) complexes bearing substituted pentane-2,4-dionate ligands. Their excellent solubility in non-polar solvents is rendered by attachment of long aliphatic chains. Our experiments on these compounds revealed their promising catalytic activity. Hence, they accelerate the autoxidation of various solvent-borne alkyd resins at much lower concentration than common for commertial **Co-Nuodex**. Furthermore, the vanadium-based driers work well at much wider range of concentrations that considerably reduces a risk of overdosing without necessity of other additives (*e.g.* through driers and auxiliary driers). The excellent performance of the vanadium-based driers at low concentrations is due to very short induction periods as revealed by kinetic studies. At concentration 0.03 wt.%, the autoxidation process starts almost immediately after coating with sufficient rate coefficient. Very promising feature of the driers is their excellent performance in long-length alkyd binder (**S60**) that suggests a great potential for ecologically sustainable paints based on high-solid systems. The detailed investigation of performance in high-solid binders including description of the interactions with other components of real paints (*e.g.* anti-skinning agents, pigments) is currently ongoing in our laboratory.

4. Experimental section

4.1 Methods and material

All syntheses were performed under nitrogen atmosphere using conventional Schlenk-line techniques. The solvents were purified and deoxygenated by standard methods. $VOSO_4 \cdot xH_2O$ (x ≈ 4) was prepared by reaction of V_2O_5 (Acros Organics) with sulfuric acid in aqueous solution and with ethanol as reduction agent [22]. The crude product was repeatedly washed by hot acetonitrile using Soxhlet extractor to remove residual sulfuric acid.

The cobalt(II) 2-ethylhexanoate (Octa-Soligen Cobalt 10 in D60, **Co-Nuodex**) was obtained from Borchers GmbH. Following solvent-borne phthalic-type alkyd resins, supplied by Spolchemie a.s., were used for both mechanical tests and kinetic measurements: alkyds modified with soybean oil CHS-Alkyd S 401 X 55 (**S40**; short oil length, acid value = 7 mg KOH/g), CHS-Alkyd S 471 X 60 (**S50**; medium oil length, acid value = 6 mg KOH/g) and CHS-Alkyd S 621W 60 (**S60**; long oil length, acid value = 7 mg KOH/g). All metal concentrations are given in wt.% based on dry matter of alkyd resin.

*4.2 Synthesis of 3-butylpentane-2,4-dione (**1a**)*

A mixture of potassium carbonate (31.0 g, 224 mmol) and potassium iodide (17.0 g, 102 mmol) in acetone (250 ml) was treated with pantane-2,4-dione (20.0 g, 200 mmol) and 1-bromobutane 27.4 g (200 mmol). The reaction mixture was heated under reflux under inert atmosphere for 48h. After cooling at room temperature, the suspension was filtered on glass frit and washed with acetone (2 × 100 ml). The volatiles were evaporated on rotavapor and the crude product was purified by vacuum distillation (75°C, 8 Torr). Yield: 15.9 g (102 mmol, 50.9 %). Anal. Calcd. for ($C_9H_{16}O_2$): C, 69.19; H, 10.32. Found: C, 69.45; H, 10.08. Spectroscopic data are in line with those published elsewhere [23].

*4.3 Synthesis of 3-hexylpentane-2,4-dione (**1b**)*

The reaction was carried out as described for 3-butylpentane-2,4-dione but with 1-bromohexane (33.0 g, 200 mmol). Crude product was purified by vacuum distillation (95°C, 6 Torr). Yield: 19.5 g (106 mmol, 52.9 %). Anal. Calcd. for ($C_9H_{16}O_2$): C, 71.70; H, 10.94. Found: C, 71.48; H, 10.65. Spectroscopic data are in line with those published elsewhere [23].

*4.4 Synthesis of 3-octylpentane-2,4-dione (**1c**)*

The reaction was carried out as described for 3-butylpentane-2,4-dione but with 1-bromooctane (38.6 g, 200 mmol). Crude product was purified by vacuum distillation (100°C, 3 Torr). Yield: 19.9 g (94 mmol, 46.9 %). Anal. Calcd. for ($C_9H_{16}O_2$): C, 73.54; H, 11.39. Found: C, 73.34; H, 11.30. Spectroscopic data are in line with those published elsewhere [23].

*4.5 Synthesis of bis(3-butylpentane-2,4-dionato)oxovanadium (**2a**)*

$VOSO_4 \cdot xH_2O$ (2.00 g, 8.51 mmol) was dissolved in water (10 ml) and treated with 3-butylpentane-2,4-dione (**1a**; 2.64 g, 16.9 mmol) and dropwise neutralized with aqueous solution of sodium carbonate. The reaction mixture was stirred at room temperature for 3 h. The crude product was extracted with dichloromethane. The volatiles and unreacted ligand were removed by the vacuum distillation on Kugelrohr. The product was recrystallized from hexane at low temperature (–30°C) and vacuum dried. Yield: 1.32 g (3.50 mmol, 41.4 %). Anal. Calcd. for ($C_{18}H_{30}O_5V$): C, 57.29; H, 8.01. Found: C, 57.02; H, 7.85. IR (ATR-C, cm^{-1}): 996 m ($\nu_{V=O}$). EPR(toluene): $|A_{iso}|$ =10.39 mT, g_{iso} = 1.948. UV-vis in CH_2Cl_2 [λ_{max}/nm (ε/$M^{-1}\cdot cm^{-1}$)]: 600 (105), 679 (108), 418 (163), 340sh (5010), 316 (13280), 285 (9260), 233 (9190).

*4.6 Synthesis of bis(3-hexylpentane-2,4-dionato)oxovanadium (**2b**)*

The reaction was carried out as described for compound **1** but with 3-hexylpentane-2,4-dione (**1b**; 3.11 g, 16.9 mmol). Yield: 1.89 g (4.36 mmol, 51.6 %). Anal. Calcd. for ($C_{22}H_{38}O_5V$): C, 60.96; H, 8.84. Found: C, 60.62; H, 8.99. IR (ATR-C, cm^{-1}): 993 m ($\nu_{V=O}$). EPR(toluene): $|A_{iso}|$ =10.39 mT, g_{iso} = 1.948. UV-vis in CH_2Cl_2 [λ_{max}/nm (ε/$M^{-1}\cdot cm^{-1}$)]: 597 (96), 679 (94), 418 (146), 341sh (4540), 318 (12630), 285 (8170), 235 (8329).

*4.7 Synthesis of bis(3-octylpentane-2,4-dionato)oxovanadium (**2c**)*

The reaction was carried out as described for compound **1** but with 3-octylpentane-2,4-dione (**1c**; 3.57 g, 16.9 mmol). Yield: 1.81 g (3.70 mmol, 43.5%). Anal. Calcd. for ($C_{26}H_{46}O_5V$): C, 63.78; H, 9.47. Found: C, 63.59; H, 9.63. IR (ATR-C, cm^{-1}): 995 m ($\nu_{V=O}$). EPR(toluene): $|A_{iso}|$ =10.37 mT, g_{iso} = 1.949. UV-vis in CH_2Cl_2 [λ_{max}/nm (ε/$M^{-1}\cdot cm^{-1}$)]: 600 (113), 675 (108), 416 (160), 341sh (4310), 318 (15540), 287 (8470), 235 (9880).

4.8 Preparation of test coatings

Relevant drier was treated with 10 µl of toluene. Immediately after dissolution, it was treated with 5.00 g of alkyd resin and stirred for 10 min to get a homogenous mixture. The films were cast on clean glass plates using frame applicators with appropriate gaps (76 µm for the film drying time, 150 µm for the film hardness and 100 µm for the *in situ* infrared experiments).

4.9 Determination of drying times

The drying performance has been determined using a BYK Drying Time Recorder. The instrument is a straight-line recorder equipped with hemispherical ended needle (5 g weight used). The needle travels the length of the test strip under standard laboratory conditions (t = 23°C, relative humidity 50%). The trace left on the film during the drying has been used to define tack free time (τ_1) and total dry time (τ_2). During the stage 1 ($t = 0–\tau_0$), the paint flows together and starts to polymerize. It gives bold and uninterrupted line. During the stage 2 ($t = \tau_1–\tau_2$), the surface is sticky and the path is ripped. After τ_2 (stage 3) the paint is through dry and needle travels on top of the surface and no trace in the film is observable [24, 25].

4.10 Determination of film hardness

Film hardness development was monitored using a Persoz type pendulum (Elcometer Pendulum Hardness Tester, UK) in conformity with ISO 1522 within 100 days. The measured value was related to the hardness of a glass standard and expressed as relative hardness. The error in determination of surface hardness was estimated to be 0.5%.

4.11 Infrared spectroscopy

The IR spectra of vanadium compounds **2a**–**2c** have been obtained using ATR technique (single-bounce diamond crystal, 32 scans per spectrum, resolution 2 cm^{-1}) on Nicolet iS50 spectrometer in the range of 4000–500 cm^{-1}. The autoxidation of alkyd resin was followed by time-resolved technique at the same spectrometer. Mixture of alkyd resin with appropriate drier was spread on the NaCl plate. Sample was placed in the spectrometer and IR spectrum was recorded each 5 min at 23°C. Collected IR spectra were integrated using a fixed two-point baseline in the region 3014–2997 cm^{-1} (*cis*-C=*C–H* stretch). Rate coefficient at the beginning of

the autoxidation process ($-k_{CH,max}$) was estimated as the steepest slope of the logarithmic plot of the integrated area *vs*. time. The intensity of band at 989 cm^{-1} was determined as the height of the band at this wavenumber using linear baseline fixed at wavenumbers 1010 and 945 cm^{-1}.

4.12 EPR spectroscopy

EPR spectra were measured on Miniscope MS 300 spectrometer in microwave X-band (~9.5 GHz). The apparatus was gauged on DPPH value (g_{iso} = 2.0036 ± 2). Fluid solutions of **2a**–**2c** were measured in glass capillaries (ID 0.5 mm) at room temperature (293 K) and the frozen solution in quartz tubes (ID 3 mm) at 123 K. The test coatings treated with vanadium-based driers were prepared by standard procedure and cured for two weeks at room temperature. Then, the coatings were scratched off and the spectra were measured in quartz tubes (ID 5 mm) at 293 K. The obtained EPR spectra were computer simulated using EPR simulation software SimFonia v.1.2 (Bruker). A second-order perturbation theory was used for description of the interaction between electronic spin and nuclear spin of vanadium. Anisotropic line-widths and mixed Lorentzian/Gaussian lines shapes were used for simulations.

4.13 UV-vis spectroscopy

Electronic absorption spectra (200–1080 nm) were run under inert atmosphere on a Black-Comet C-SR-100 concave grating spectrometer equipped with a dip probe having an optical pathway of 10 mm.

4.14 X-ray crystallography

Crystallographic data for **2a**–**2c** were collected on Nonius KappaCCD diffractometer equipped with Bruker APEX-II CCD detector by monochromatized MoKα radiation (λ = 0.71073 Å) at a temperature either 200 K (**2a**) or 150(2) K (**2b** and **2c**). The structures were solved by direct methods (XT) [26] and refined by full matrix least squares based on F^2 (SHELXL2014) [27]. The absorption corrections were carried on using multi-scan method. The most of hydrogen atoms were found on difference Fourier map and all were recalculated into idealized positions. All hydrogen atoms were refined as fixed (riding model) with assigned temperature factors $H_{iso}(H)$ = 1.2 U_{eq}(pivot atom) or 1.5 U_{eq} for methyl moiety. The disorders of the end of one carbon chain in crystals **2a** and **2c** were described by the splitting of atomic positions with refined corresponding occupational factors. The crystal **2a** was measured at 200 K since at lower temperature underwent phase transition accompanied with the destruction of single crystal. The volume of resulting unit cell at 150 K is three times of unit cell at high temperature, with three symmetrically independent molecules; however, one of them remains disordered. Therefore, the structure **2a** of high temperature phase is presented.

Appendix A. Supplementary data

CCDC 1520217–1520219 contain the supplementary crystallographic data for **2a**, **2b** and **2c**, respectively. These data can be obtained free of charge via http://www.ccdc.cam.ac.uk/conts/retrieving.html, or from the Cambridge Crystallographic Data Centre, 12 Union Road, Cambridge CB2 1EZ, UK; fax: (+44) 1223-336-033; or e-mail: deposit@ccdc.cam.ac.uk.

Acknowledgements

This work was supported by Ministry of Education of the Czech Republic (Project No. UPA SG360011).

References

[1] D. Nelson, Paint and Coating Testing Manual: 15th Edition of the Gardner-Sward Handbook (Ed.: J. V. Koleske), ASTM International, West Conshohocken, **2012**, pp. 65–71.
[2] M. D. Soucek, T. Khattab, J. Wu, Prog. Org. Coat. 73 (2012) 435–454.
[3] R. van Gorkum, E. Bouwman, Coord. Chem. Rev. 249 (2005) 1709–1728.
[4] E. Bouwman, R. van Gorkum, J. Coat. Technol. Res. 4 (2007) 491–503.
[5] Z. O. Oyman, W. Ming, R. van der Linde, Appl. Catal. A 316 (2007) 191–196.
[6] J. Z. Wu, E. Bouwman, J. Reedijk, Prog. Org. Coat. 49 (2004) 103–108.
[7] Z. O. Oyman, W. Ming, F. Micciche, E. Oostveen, J. van Haveren, R. van der Linde, Polymer 45 (2004) 7431–7436.
[8] Ö. Gezici-Koc, C. A. A. M. Thomas, M. E. B. Michel, S. J. F. Erich, H. P. Huinink, J. Flapper, F. L. Duivenvoorde, L. G. J. van der Ven, O. C. G. Adan, Mater. Today Commun. 7 (2016) 22–31.
[9] J. W. de Boer, P. V. Wesenhagen, E. C. M. Wenker, K. Maaijen, F. Gol, H. Gibbs, R. Hage, Eur. J. Inorg. Chem. (2013) 3581–3591.
[10] B. Pirš, B. Znoj, S. Skale, J. Zabret, J. Godnjavec, P. Venturini, J. Coat. Technol. Res. 12 (2015) 965–974.
[11] M. Erben, D. Veselý, J. Vinklárek, J. Honzíček, J. Mol. Catal. A: Chem. 353-354 (2012) 13–21.
[12] O. Preininger, J. Vinklárek, J. Honzíček, T. Mikysek, M. Erben, Prog. Org. Coat. 88 (2015) 191–198.
[13] O. Preininger, J. Honzíček, P. Kalenda, J. Vinklárek, J. Coat. Technol. Res. 13 (2016) 479–487.
[14] R. Hage, J. W. de Boer, K. Maaijen, Inorganics 4 (2016) 11.
[15] D. C. Crans, K. A. Woll, K. Prusinskas, M. D. Johnson, E. Norkus, Inorg. Chem. 52 (2013) 12262–12275.
[16] E. Shuter, S. J. Rettig, C. Orvik, Acta Cryst. C51 (1995) 12–14.
[17] S. S. Amin, K. Cryer, B. Zhang, S. K. Dutta, S. S. Eaton, O. P. Anderson, S. M. Miller, B. A. Reul, S. M. Brichard, D. C. Crans, Inorg. Chem. 39 (2000) 406–416.
[18] W. T. Elliott, Surface Coatings: Volume 1 Raw Materials and Their Usage, Chapman & Hall, London, **1993**, pp. 76-109.
[19] S. T. Warzeska, M. Zonneveld, R. van Gorkum, W. J. Muizebelt, E. Bouwman, J. Reedijk, Prog. Org. Coat. 44 (2002) 243–248.
[20] F. R. van de Voort, A. A. Ismail, J. Sedman, G. Emo, J. Am. Oil Chem. Soc. 71 (1994) 243–253.
[21] Z. O. Oyman, W. Ming, R. van der Linde, Prog. Org. Coat. 48 (2003) 80–91.
[22] G. Brauer, Handbuch der Präparativen Anorganischen Chemie, Stuttgart, **1962**.
[23] A. O. Terent'ev, V. A. Vil', I. A. Yaremenko, O. V. Bityukov, S. O. Levitsky, V. V. Chernyshev, G. I. Nikishin, F. Fleury, New J. Chem. 38 (2014) 1493–1502.
[24] F. Micciche, E. Oostveen, J. van Haveren, R. van der Linde, Prog. Org. Coat. 53 (2005) 99–105.
[25] O. Preininger, J. Honzíček, J. Vinklárek, M. Erben, Prog. Org. Coat. 77 (2014) 292-297.
[26] G. M. Sheldrick, Acta Cryst. C71 (2015) 3–8.
[27] G. M. Sheldrick, SHELXL2014/7, University of Göttingen, Germany (2014).